REGULAR PAPER

Design and Investigation of a Novel Point Absorber on Performance Optimization Mechanism for Wave Energy Converter in Heave Mode

Tri Dung Dang[1] · Cong Binh Phan[1,2] · Kyoung Kwan Ahn[3]

Abstract

Nowadays, wave energy plays an important role in renewable energy resource. In over 30 years, several researches in wave energy converter system (WEC) have been deployed and carried out. This paper proposes a new mechanism to achieve the resonant behavior of a point absorber floating buoy type of WEC system with mechanical power take-off. The original WEC system uses the bidirectional gearbox to convert up and down motion of the wave in heave mode to one-way rotation. By designing the array of hydraulic springs, the equivalent stiffness of the float can be reduced to close to the relatively low frequency of the wave. Then the buoy is at near resonance with the wave, also increase the power capture bandwidth and the performance of the operating system. In this paper, the specification of the system is proposed and studied. The working principle is analyzed. The mathematical model is then derived to investigate the operation. Experiments are performed to validate the simulation results based on mathematical model. Numerical simulation using Matlab/Simulink has been done to evaluate the effectiveness of the new control stiffness mechanism.

Keywords Wave energy converter (WEC) · Point absorber · Mechanical power take-off (PTO) · Bidirectional gearbox (BG) · Stiffness spring mechanism

1 Introduction

On the purpose of reducing environment pollution and dealing with the conflicts of the depletion of the fossil fuel resource, the alternatives renewable energy resources have been urgently searched for over decades. The ocean waves which are performed by wind and hence are indirect form of solar energy are the most promising form of the ocean energy. Besides, the wave energy density is about ten times higher than solar and five than wind [1], ocean wave has high utilization time, predictable properties and costless in fuel so that it is considered as the most potential source to solve energy crisis.

Wave energy converter (WEC) is known as the device system which has the possibility of converting wave energy into a different kind of usable source, i.e. electricity. The number of studies and researches about WEC has been being rapidly increasing since 1970s. Several methods and technologies have been proposed and numerous prototypes have been deployed in real sea. Irade and Falcão presented their own reviews on wave energy technologies and WEC systems also. WEC have various types, shapes, sizes and methods. Both Irade and Falcão indicated that we can classify WEC according to three characteristics: by location (onshore, nearshore and offshore) or by size (attenuator, terminator and point absorber) or by working principle (three main configurations of WEC are based on overtopping devices, oscillating water column and oscillating body system) [1, 2].

Floating buoys which are known as oscillating body system and frequently conceived as point absorber (i.e. its diameter in horizontal direction is significantly smaller in comparison to wavelength) are received more attention for use in WEC [1]. Whose heaving oscillation in waves can be used to extract wave energy for electricity generation. It is one of the simplest wave energy converters from the hydrodynamic perspective [3]. Under wave form motion, a device

✉ Kyoung Kwan Ahn
  kkahn@ulsan.ac.kr

1 Graduate School of Mechanical Engineering, University
   of Ulsan, Nam-gu, Ulsan 44610, South Korea

2 Faculty of Mechanical Engineering, Ho Chi Minh
   City University of Technology and Education,
   Ho Chi Minh City 700000, Vietnam

3 Department of Mechanical Engineering, University of Ulsan,
   Nam-gu, Ulsan 44610, South Korea

is forced to move up and down in a bobbing or pitching motion. Then, the movements of these devices can be easily transmitted into a rotary or linear motion of the generator to generate electricity.

Several studies have been carried out on the point absorber types [4–16] to indicate the performance and the power absorption of WEC. Point absorber includes three main power take-off (PTOs) type to absorb energy from waves. The first type is direct drive devices using linear generators [5, 9, 13], whose large permanent magnets can be costly and there is no provision for any energy storage to smooth the output. The second type involves hydraulic devices [4, 7, 8, 12], in which the motion of the buoy is converted to drive hydraulic actuators. A hydraulic motor driven by the hydraulic actuator is then employed to drive a conventional electric generator. In this type, too many components cause low efficiency and care must also be taken with closed-loop devices to prevent leaks of hydraulic oil into the surrounding environment. The third type involves purely mechanical structure devices, which typically offers high conversion efficiencies and allow for simpler generators (rotational instead of linear) to be used. Thus, this paper presents a WEC with new mechanical PTO design with simple structure and high efficiency to convert wave energy to electrical energy.

The problem of maximizing the extraction energy has been dealt either by suitably choosing the hydrodynamic and mechanical characteristics of the devices to achieve resonant motion or by applying specific control strategies to properly guide the motion of the floating buoy [6]. The second approach includes several methods as latching control (known as phase control) which firstly proposed by Falnes [17, 18], French [19] and Guenther [20] or declutching control presented by Falcao [21]. Both methods in second approach are required a predictive model which can be found similarly in Refs. [22, 23].

According to Falnes in Ref. [24], the maximum energy absorption can be achieved by bringing the natural frequencies to resonance with the incident waves and controlling the resistive load from the PTO system. The natural frequency of the regular WEC systems ω_n can be calculated by:

$$\omega_n = \sqrt{\frac{K_{eq}}{m_b + m_{\infty,heave}}} = \sqrt{\frac{S_b + K_{add}}{m_b + m_{\infty,heave}}} \quad (1)$$

where K_{eq} is the equivalent stiffness, m_b is the buoy mass, $m_{\infty,heave}$ is the infinitely added mass for the heave coordinate, S_b is the hydrostatic stiffness of the buoy and K_{add} is the additional stiffness.

To match the relatively low frequency of the wave ω_v, either the mass of the buoy must be increased, or the stiffness of the buoy must be decreased. As investigated and

indicated in conclusion by Garnaud in Ref. [3], compared with a single large buoy built with the same amount of material, the compact array of small buoy is potentially more efficient in natural seas. Therefore, this work considered reducing the stiffness of the floating buoy by modifying the structure of the float. By designing the array of hydraulic springs, the equivalent stiffness of the float can be reduced to match the relatively low frequency of the wave. So that the buoy is at resonance with the wave, also achieve the highest performance of the operating system.

In this paper, the high efficiency WEC is presented to investigate the performance under some regular waves. Then, the development of the presented WEC is carried out by coupling the current system with the stiffness control system. Analytical model is built in Matlab/Simulink by using the wave linear theory. The simulation results are compared with that of the basic WEC system. Finally, an PID controller is designed to control the stiffness so that the developed WEC can capture wave power with the highest efficiency.

2 Design Concept and Working Principle

Oscillating bodies can be floating, semi-submerged or fully submerged, the last type is rarely considered [2]. This study focuses on a hemisphere floating buoy type which is shown as Fig. 1. This buoy is small in comparison to incident wavelength then it is also called a point absorber. Figure 1 shows the schematic of the proposed WEC which consists of three main components: a hemi-sphere floating buoy; a power take-off system which includes a rack and pinion mechanism, a bidirectional gearbox (BG) coupled with a flywheel and an electric generator; a control stiffness mechanism (CSM) which includes four hydraulic cylinders inside the hemi-sphere connected with a hydraulic accumulator via pipeline inside the main shaft, both are connected to a pressure control unit.

Original high efficiency WEC and its working principle had also been proposed in Ref. [11]. Under wave motion, the buoy and the main shaft are forced to oscillate up and down together in vertical z direction along a rigid frame. The main shaft is coupled with the BG by the rack and pinion gear mechanism which are illustrated in Fig. 1. The upward and downward motion of the floating buoy is transferred to one-way rotation of the output shaft thanks to two one-way bearings. Two pinions are fixed to two input shafts that are coupled with two driving gears. The two driving gears are engaged with the driven gear to convert bidirectional motion into one-way rotary motion. Then, the output shaft of the BG is fixed to the driven gear. The flywheel is used to store and release rotational energy, which keeps the speed of the output shaft smoother. Finally, the electric generator driven by speed of the output shaft generates the electricity.
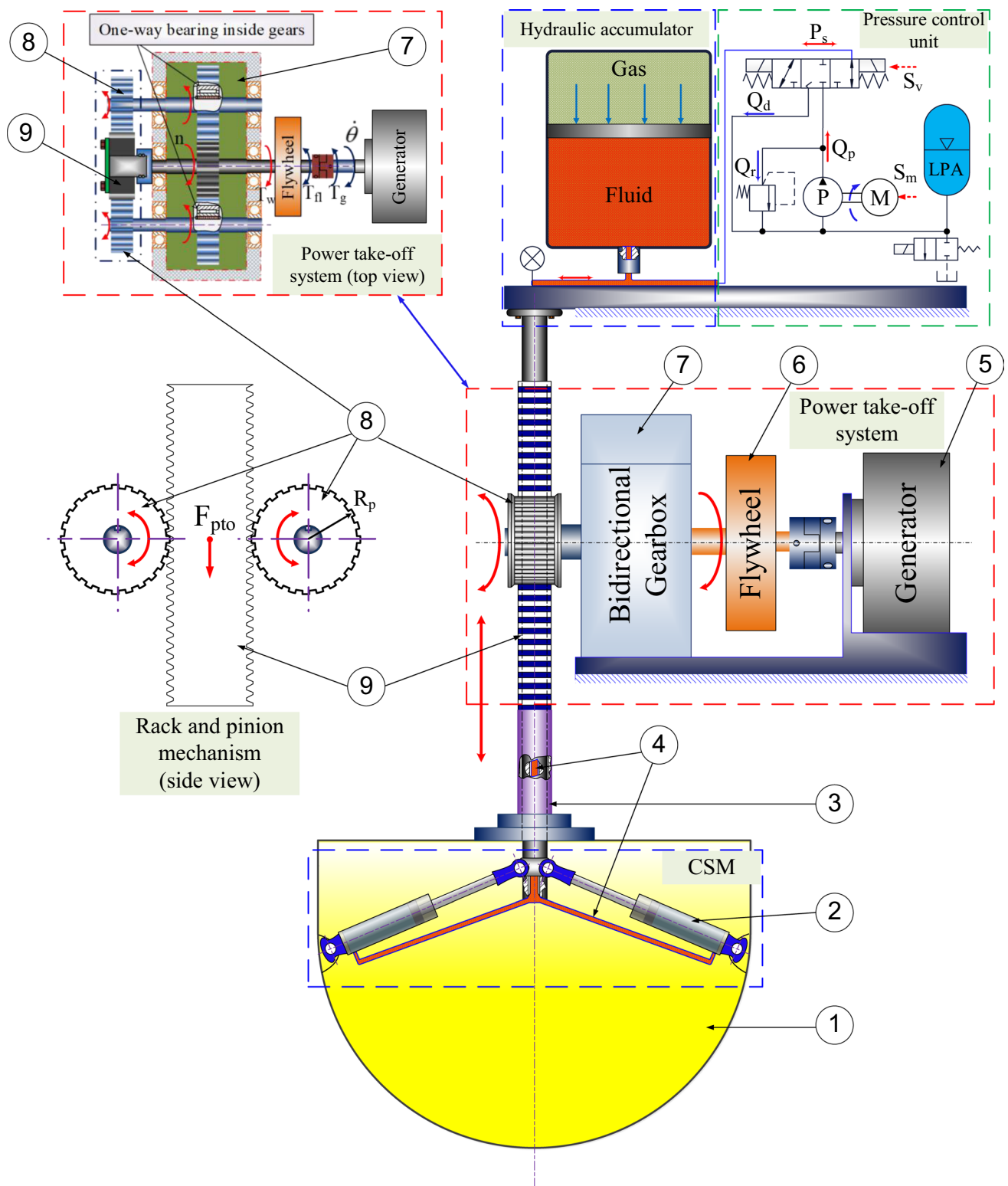
Fig. 1 Configuration of the WEC with the control stiffness mechanism (CSM): 1-floating buoy; 2-hydraulic cylinder; 3-main shaft; 4-fluid pipe; 5-generator; 6-flywheel; 7-bidirectional gearbox; 8-pinions; 9-rack

The CSM includes two parts: a set of four cylinders inside the buoy and a pressure control system. Four cylinders are arranged perpendicular with others to provide a balance force in vertical direction. The working principle is illustrated by Fig. 2. With a displacement of the buoy in the vertical direction, the fluid pressure inside four cylinders provides a vertical spring force. This force counteracts the hydrostatic heave force so that it decreases the equivalent stiffness of the WEC. Then the natural frequency of the device can be tuned to close to the wave frequencies. Besides, the width capture ratio is increasing thanks to resonance condition. This working principle is similar to that used in the negative stiffness system [25]. The pressure control unit includes an electrical motor-hydraulic pump M-P combination with a control valve S_V to pump high pressure fluid Q_P into four cylinders, a high-pressure accumulator (HPA) to maintain the pressure P_S in the circuit, a relief valve for safety and a low-pressure accumulator (LPA) for energy saving purpose.

3 Dynamics Modelling

The general dynamics of the WEC can be described by the motion of floating buoy under the effect of the hydrodynamic force F_h, the resistance force F_{pto} due to the PTO system and the spring forces of the cylinders F_{sf}. In this paper, the WEC behavior is simulated in time domain and regular waves. This is the main limitation of the model since irregular wave inputs would be more accurate and more realistic. However, the difference is limited, at least for short waves

[13]. Therefore, the simplified model of regular waves is acceptable and chosen.

The study of the mathematical model was discussed in detail in the previous work [11]. The floating buoy dynamics are obtained by solving the following equation:

$$m_b \ddot{z} = F_h + F_{pto} + F_{sf} \tag{2}$$

where z is the vertical displacement of the buoy.

3.1 Hydrodynamic Model

In time domain, the simplified hydrodynamic force F_h acting on the buoy which combines the excitation force F_e, the radiation force F_r, the viscous force F_v and the hydrostatic restoring force F_s is calculated by the following equations:

$$F_h = F_e + F_r + F_v + F_s \tag{3}$$

$$F_e = f_e \frac{H}{2} \sin(\omega t + \alpha) \tag{4}$$

$$F_r = -M_a \ddot{z} - R_r \dot{z} \tag{5}$$

$$F_v = -\frac{1}{2} \rho C_d A_d (\dot{z} - \dot{\eta}) |\dot{z} - \dot{\eta}| \tag{6}$$

$$F_s = -\rho g A_d z = -S_b z \tag{7}$$

The excitation force which can be evaluated by WAMIT [26] directly, where f_e is the excitation force coefficient; H and ω are the wave height and frequency and α is the phase angle between the wave and the induced heaving force.
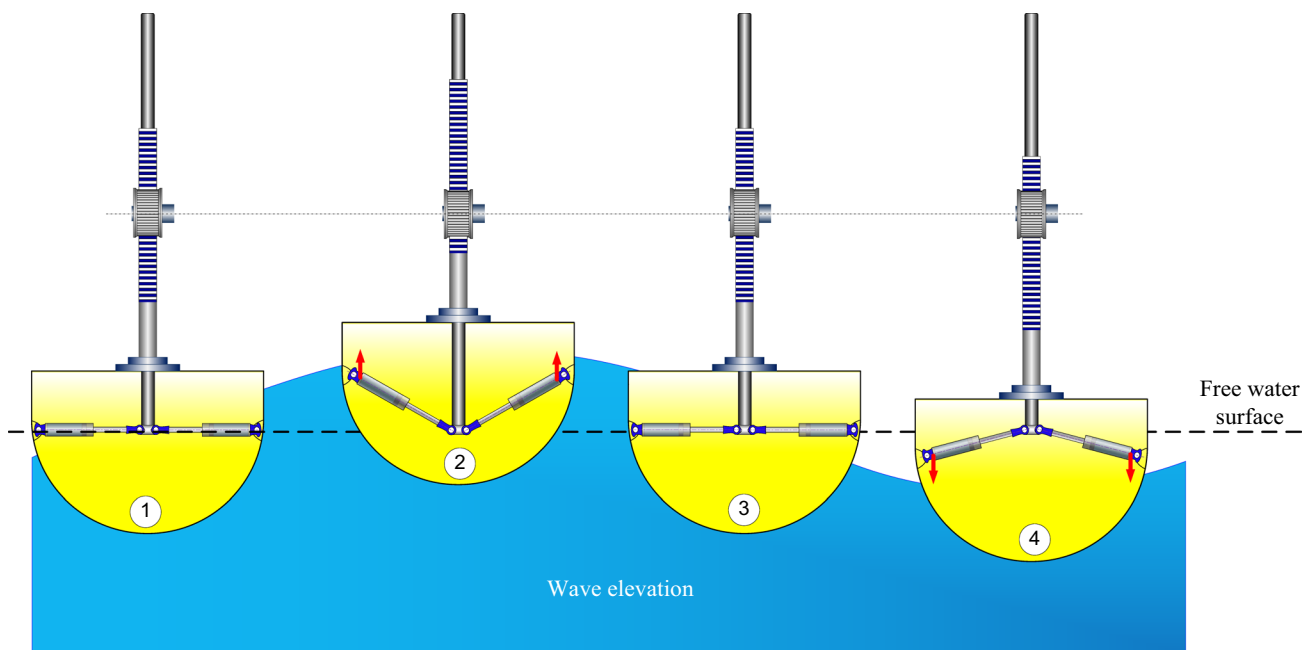

Fig. 2 WEC behavior under wave elevation: at equilibrium position (1) and (3), upward motion (2) and downward motion (4)

The radiation force is the required force to move the floating buoy. It is commonly decomposed into two components: the added inertial force, due to the water volume moving with the floating buoy, and the radiation damping force, due to the induced wave by the floating buoy oscillations where M_a is the added mass and R_r is the radiation damping coefficient which can be evaluated with WAMIT.

The viscous effects can be modeled similar to the drag term where ρ is sea water density C_d is the drag coefficient, A_d is the characteristic frontal area which depends on the body area projected on the water plane, and $\dot{\eta}$ is the vertical velocity of the free water surface.

The hydrostatic force which is governed by Archimedes' Principle and it is the difference between the volume of displaced water where ρ is the gravitational acceleration, S_b is the buoyancy (hydrostatic) stiffness.

3.2 PTO Model

For simplicity, the resistive force from the PTO system can be comprised of two components: friction force and resistive force from the generator, which is presented in the following equation:

$$F_{pto} = F_f + F_u \tag{8}$$

where F_f represents the mechanical friction and viscous forces acting on the floating buoy.

The resistive force from the generator F_u is only taken into account when the instantaneous speed of the input shaft n, caused by the velocity of the floating buoy, is larger than the generator speed $\dot{\theta}$. Otherwise, in reversely, there is no resistant force on the buoy. The resistive force can be calculated by:

$$F_u = \begin{cases} \frac{T_g + T_{fl}}{r_p} k_g & for \ \dot{\theta} \leq n \quad where \quad n = \frac{\dot{z}}{r_p} k_g \\ 0 & for \ otherwise \end{cases} \tag{9}$$

where T_g is the resistive torque from the generator and T_{fl} is the torque from the flywheel, r_p is the radius of the pinion, k_g is the ratio of the bidirectional gear.

3.3 The Control Stiffness Mechanism Model

When the buoy position higher than the calm free water surface (second buoy in Fig. 2), the force diagram is shown as Fig. 3 where R is the buoy radius. The high pressure inside the cylinder causes a force F_{cyl} along the cylinder axis. The horizontal element F_x of this force is eliminated due to the other cylinder in the opposite side. Only the vertical element affects the movement of the buoy. The total force applies on
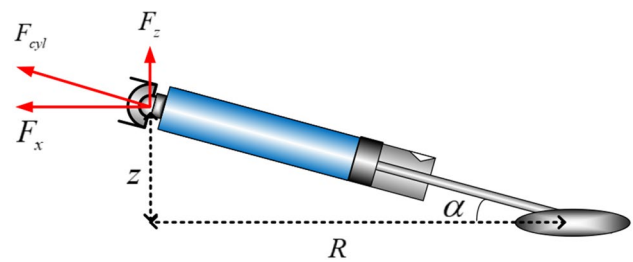

Fig. 3 The cylinder spring force counteracts the hydrostatic force

the buoy in heave motion is the sum of all four cylinders' forces:

$$F_{sf} = 4F_z = 4F_{cyl} \sin \alpha = 4PA_c \sin \alpha = 4PA_c \frac{z}{\sqrt{z^2 + R^2}} \tag{10}$$

where P is the cylinder pressure, A_c is the piston area.

As seen in above equation, this force is also a function of the buoy this displacement like the hydrostatic force F_S. Since these forces are in the opposite sign the cylinders forces counteract the hydrostatic force. Then it decreases the equivalent stiffness of the buoy.

3.4 Energy Conversion

Below are the equations for calculating the generated power and energy of WEC, respectively. The power is equal to the multiplication of the generator resistive force and speed. The energy is integral of power over time. These equations are used to evaluate the improvement of the system with and without the control stiffness mechanism by calculating the values in both cases.

$$P_g = T_u \dot{\theta} \tag{11}$$

$$E_g = \int_0^t P_g dt \tag{12}$$

4 Test Rig Setup and Model Verification

In order to verify the analytical model of basic WEC, the test rig was fabricated and setup at the Research Institute of Small and Medium Shipbuilding (RIMS), Busan, Korea.

The schematic diagram of the whole system is shown in Fig. 4. The main components include a wave maker; the buoy coupled with the PTO system (via the rack and pinion mechanism) consists of the BG module, which is comprised of a guide line system, the rack and pinion gear mechanism, the flywheel and a load simulator in the test rig as shown in Fig. 5. In this paper, a magnetorheological (MR) brake
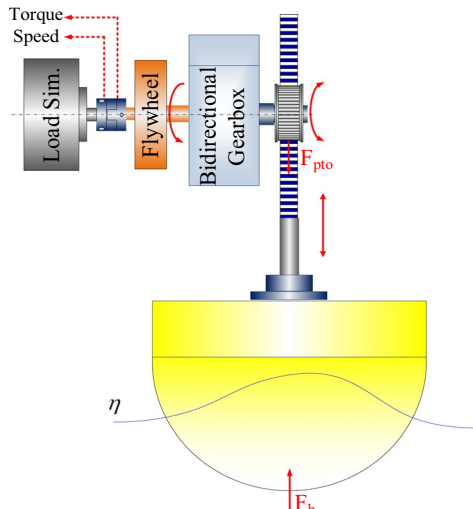
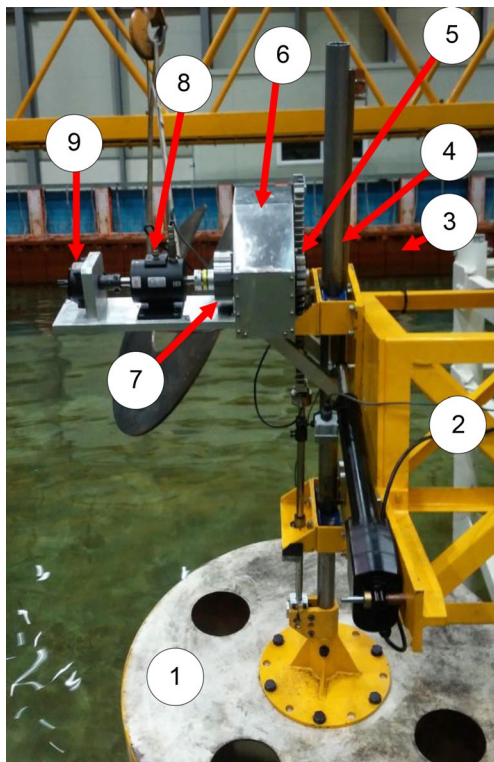**Fig. 4** The structure of experiment test rig

Fig. 5 The completed test layout of the PTO deployed in the wave tank: 1—hemi-sphere buoy; 2—rigid frame; 3—wave maker; 4—main shaft; 5—rack and pinions; 6—bidirectional gearbox; 7—flywheel; 8—torque sensor; 9—load simulator

Table 1 Setting PTO parameters for testing

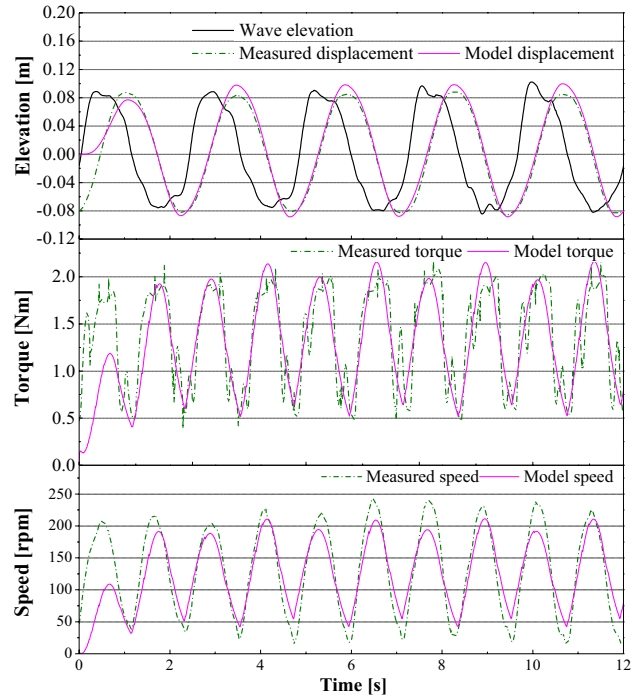| Specifications	Parameters
Buoy radius R (m)	0.6
Buoy mass m_b (kg)	178
Pinion radius r_p (m)	0.05
Gearbox ratio k_g	4
Fly. inertia I (kg m²)	0.175
Water depth h (m)	1.2

Fig. 6 Comparisons between model and experimental results

Table 2 Different wave conditions for testing

Specifications	H (m)	ω (rad/s)
Case 1	0.096	3.142
Case 2	0.150	2.618
Case 3	0.156	2.244

is used to represent the generator since it can be adjusted the load or the driven torque easily in the experiment. MR brake's working principle is based on the MR-fluid characteristic. The MR Fluid in magnetic field will apply a torque to the output shaft. The MR brake is then close-loop controlled to simulate the induced torque by the electric generator, and these values can be adjusted responding to the resistive coefficient. The induced torque and speed of the MR brake are measured using the torque transducer along with speed sensor MP-981 continuously. The estimation of the friction parameters and some required coefficients is performed in the previous work [11]. A load cell is installed on the floating buoy kept stationary relative to the platform. At
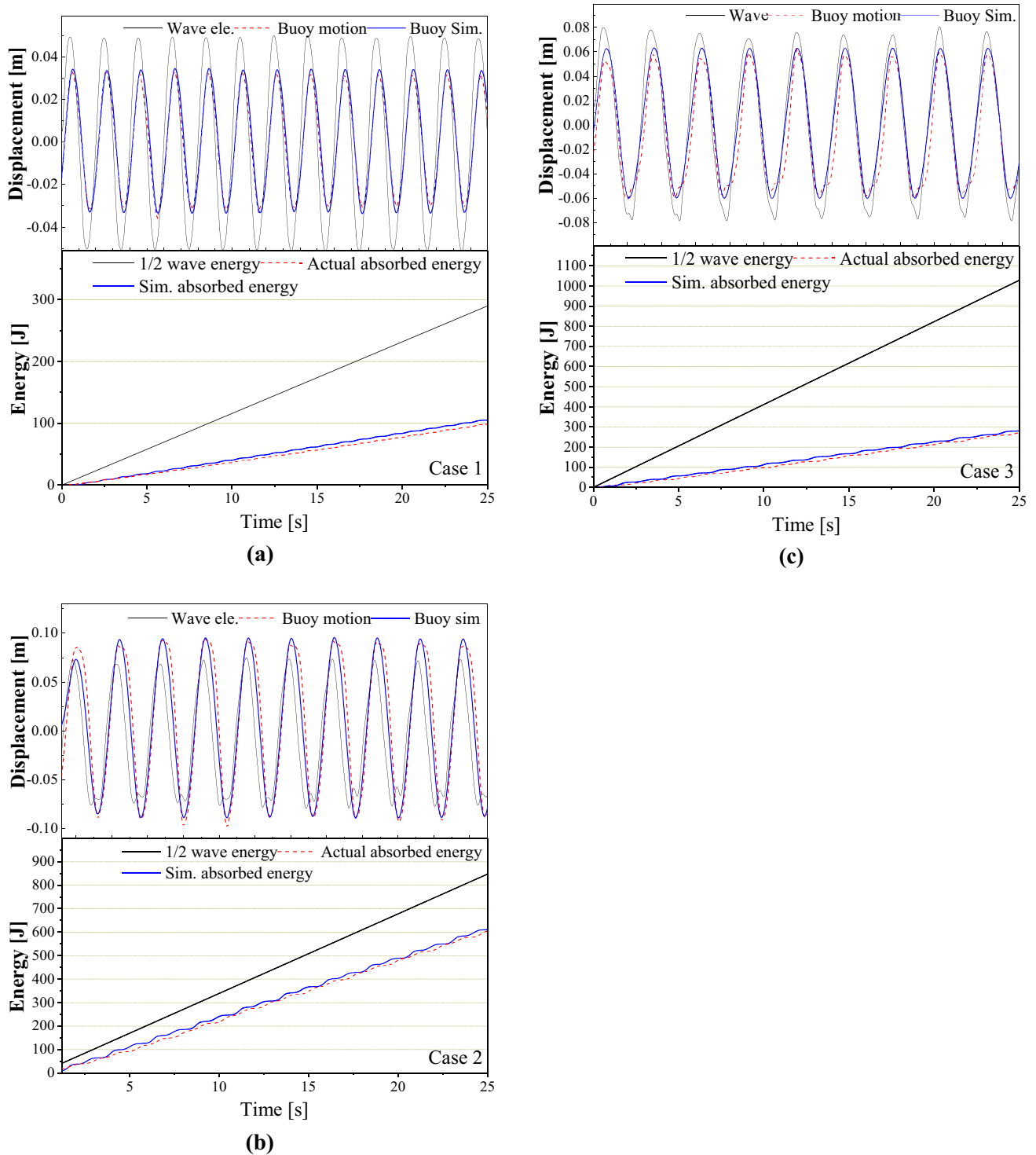
Fig. 7 The wave elevation, measured values and simulation values of buoy motion and energy under: **a** case 1; **b** case 2; **c** case 3

the equilibrium position of the buoy relative to free water surface, the load cell is calibrated to zero. A water level sensor is placed in phase with the floating buoy.

Some specifications of the test rig are measured and shown in Table 1: the buoy radius, the buoy mass, the radius of the pinion, the ratio of the BG, the flywheel

Table 3 Different conditions for simulations

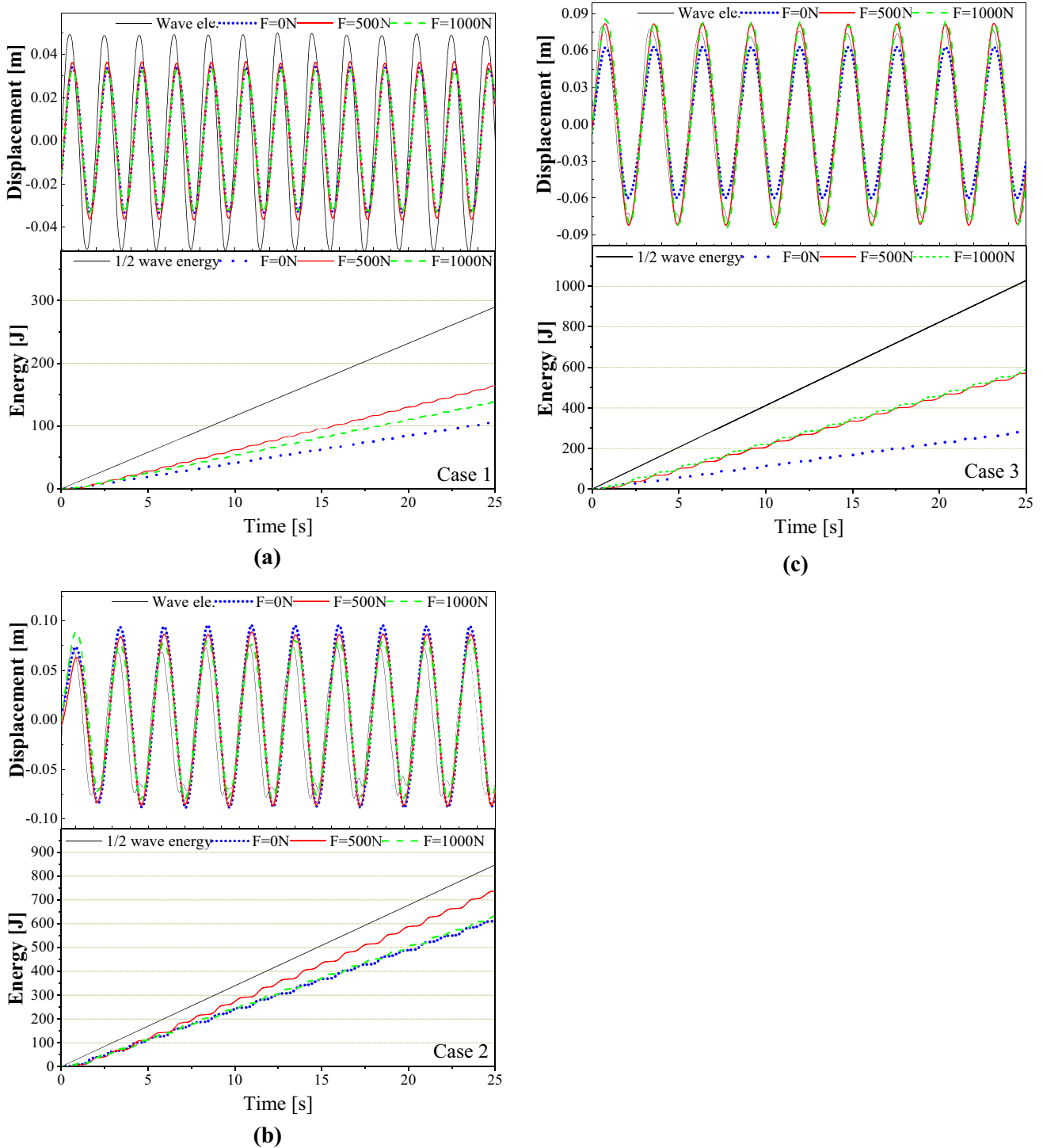| Specifications	Parameters
Cylinder diameter—D	0.05 (m)
Initial pressure—P_0	0; 10; 20 (bar)
Cylinder force—F_{cyl}	0; 500; 1000 (N)

Fig. 8 The wave elevation, buoy motion and absorbed energy under different spring forces in: **a** case 1; **b** case 2; **c** case 3

rotational inertia and water depth, respectively. Based on the geometry of the buoy, the draft, the initial conditions and the hydrodynamic parameters were obtained by using WAMIT. The hydrodynamic parameters for wave frequency which include the added mass, the radiation damping, the

excitation coefficient and the phase angle are obtained in previous work [11] also.

Experiments are carried out and compared with simulation results in Fig. 6. The actual test and model of the buoy displacements are plotted on the top of this figure,
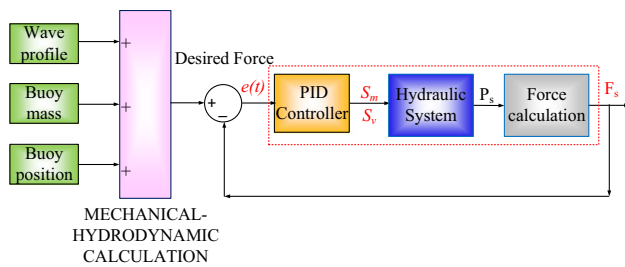
Fig. 9 Schematic control diagram for optimal spring force

meanwhile the generated torque and speed are depicted on the middle and bottom of the figure, respectively. It can be seen that the magnitude of the actual buoy oscillations is in reasonable agreement with the model. Despite some unstable positions of measured torque, probably due to non-linear wave hydrodynamic behavior, the frictional forces or imprecise mechanical parts, the mean value is approximated with the model.

5 Simulations and Results

The simulations are performed to validate the effectiveness of the system. First, the wave parameters for the three case studies are shown in Table 2. The test rig is run under three different wave conditions then the experimental results are collected and plotted in Fig. 7. These tests data are recorded in 25 s at steady state of working condition. Wave elevations and the buoy displacements are measured and plotted on the top of the figures. Then, haft of the mean wave energy, which is maximum absorbed energy in heave mode motion [27], and the generated energy are calculated and plotted on the bottom floor. The generated energy which is defined by integrating the generated power over the working time. The influence of the wave profiles on dynamic behavior of the buoy can be found these figures. Percentage change in elevation of the buoy compared to wave is about 60% in case 1, 120% in case 2 and 80% in case 3. Probability, the natural frequency of the PTO system is closer to the wave frequency in case 2 (resonance behavior) than the others. Moreover, the selection of the resistive load values has an effect on the buoy motion and the generated energy. The resistive load in case 2 is optimally chosen while in case 1 and 3 the resistive loads are not optimal values. This setup is proposed to compare the effectiveness of the proposed mechanism in both high and low efficiency cases. These results are also discussed in previous work [11]. Therefore, the test results indicate the influence of the wave profiles and resistive load on the dynamic performance of the PTO system significantly. Then, the simulation results based on the explained mathematical model for three cases are also plotted in the

same figure. This simulation results did not include the control stiffness mechanism model yet. The simulation results of buoy motion and energy absorbed in three cases indicates the reasonable agreement of the model with the real system.

Next, the new WEC concept with the addition model of the control stiffness mechanism is applied to the simulation model to verify the improvement of the proposed design. The simulation parameters for the CSM are shown in Table 3. The initial pressure inside the cylinders is set at 0, 10 and 20 bar. The zero value implies that the CSM take no effect. These pressure values are quite small in hydraulic system. It means the power consumption is insignificant. Spring forces along the cylinder axis which are calculated by the multiplication of pressure and the cylinder area are 0, 500 and 1000 N, respectively. The new simulation results of the new WEC are shown in Fig. 8. The buoy displacements under three different forces are plotted on the top of the figure and the absorbed energies are plotted on the bottom, also. The results show that in all three cases the buoy elevation and the absorbed energies when forces are applied to the cylinders usually increase much more than those in normal case ($F_{cyl} = 0$). It means the system bandwidth is larger and the buoy can absorb more energy. The performance of WEC system is different under different wave profiles and the absorbed power is not proportional to the cylinder force. In case 1, Fig. 8a shows that in both force cases the powers increase but the power is higher when $F_{cyl} = 500\,N$ than when $F_{cyl} = 1000\,N$. It seems that the optimal value for F_{cyl} in case 1 is closer to 500 N. This is also true for case 2 though the energy does not increase significantly when $F_{cyl} = 1000\,N$. While in case 3, the performance under both force values are quite similar. Result in Fig. 8c implies that the optimal value for F_{cyl} in this case is in the range of 500–1000 N.

These results show that it requires a method to choose the optimal value of the spring force. Therefore, the control strategy is presented to achieve the suitable force value. Figure 9 illustrates the schematic control diagram for optimal spring force. Since the wave profile, buoy mass and buoy position are determined, the hydrodynamic parameters are computed. Then the desired force is given. The force close-loop control is applied to control the signal S_m and S_v which are owing to control the flow rate and valve operation of the pressure control unit. Based on that, the corresponding pressure value is obtained and controlled. Consequently, the optimal force is obtained and the performance of the wave energy converter system is improved.

Simulations with the optimal spring force control are performed to evaluate the performance of the control method. The results are shown in Fig. 10. The buoy elevations and energies under the optimal force value are plotted and compared to the highest power in each case: $F_{cyl} = 500\,N$ in case 1, 2 and $F_{cyl} = 1000\,N$ in case 3. In case 2 and 3, the optimal
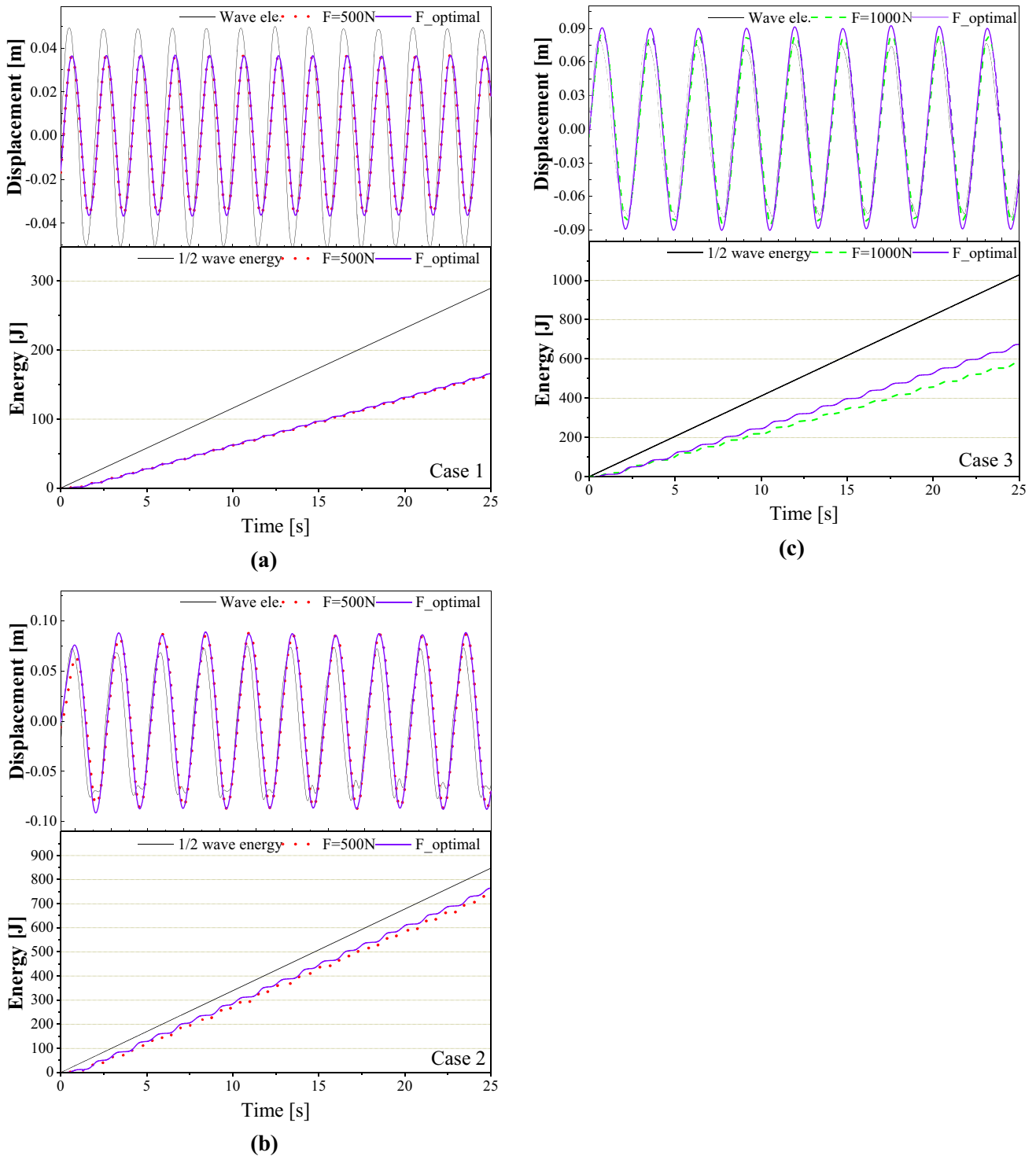
Fig. 10 The buoy motion and absorbed energy under optimal spring force in: **a** case 1; **b** case 2; **c** case 3

force value brings the system natural frequency close to the wave frequency then the absorbed energies increase significantly. While in case 1 the optimal value is approximately equal to 500 N. It can be explained that the vertical net force is a function of $\frac{z}{\sqrt{z^2+R^2}}$ while in case 1 the buoy displacement

z is quite smaller than other cases. Then the change in the cylinder force slightly affect the change in the net force value F_{sf}. Table 4 shows the improvement of the system performance under the CSM with respect to the original system. The absorbed energies in all three cases increase

Table 4 Comparisons of energy absorption

Energy absorption (J)	Without CSM (J)	With CSM (J)	Increasing amount (%)
Case 1	98.26	165.86	169
Case 2	604.25	764.91	127
Case 3	271.57	674.02	248

significantly. Especially in case 1 and 3 while the system efficiencies are low due to non-optimal resistive load values. These results express the effectiveness of the proposed mechanism.

6 Conclusions

This paper develops a new mechanism for the extraction of ocean wave energy converter. The specification of the WEC and the control stiffness mechanism are proposed and studied. The working principle is analyzed. The mathematical model is then derived in order to investigate the system operation. Numerical simulation using Matlab/Simulink has been done to evaluate the performance of the system. The performances of the actual test are in reasonable agreement with that of model. With the new mechanism, the natural frequency of device can be tuned to close wave frequencies. Then, the width capture ratio is increasing thanks to resonance condition. Consequently, the WEC can absorb significantly more wave energy. The future works will focus on two following aspects: study on the prediction problem of wave profile and investigate the performance of the proposed WEC in irregular waves to adapt with the realistic conditions.

References

1. Iraide, L., Jon, A., Salvador, C., de Iñigo Martínez, A., & Iñigo, K. (2013). Review of wave energy technologies and the necessary power-equipment. *Renewable and Sustainable Energy Reviews, 27,* 413–434.
2. Falcão, A. F. O. (2010). Wave energy utilization: A review of the technologies. *Renewable and Sustainable Energy Reviews, 14,* 899–918.
3. Garnaud, X., & Mei, C. C. (2010). Comparison of wave power extraction by a compact array of small buoys and by a large buoy. *IET Renewable Power Generation, 4,* 519–530.
4. Vantorre, M., Banasiak, R., & Verhoeven, R. (2004). Modelling of hydraulic performance and wave energy extraction by a point absorber in heave. *Applied Ocean Research, 26,* 61–72.
5. Bostrom, C., & Leijon, M. (2011). Operation analysis of a wave energy converter under different load conditions. *IET Renewable Power Generation, 5,* 245–250.
6. Mavrakos, S. A., & Katsaounis, G. M. (2010). Effects of floaters' hydrodynamics on the performance of tightly moored wave energy converters. *IET Renewable Power Generation, 4,* 531–544.
7. Ahn, K. K., Truong, D. Q., Tien, H. H., & Yoon, J. I. (2012). An innovative design of wave energy converter. *Renewable Energy, 42,* 186–194.
8. Truong, D. Q., & Ahn, K. K. (2014). Development of a novel point absorber in heave for wave energy conversion. *Renewable Energy, 65,* 183–191.
9. Binh, P. C., Truong, D. Q., & Ahn, K. K. (2012). A study on wave energy conversion using direct linear generator. In *12th international conference on control, automation and systems*.
10. Binh, P. C., Nam, D. N. C., & Ahn, K. K. (2015). Design and modeling of an innovative wave energy converter using dielectric electro-active polymers generator. *International Journal of Precision Engineering and Manufacturing, 16,* 1833–1843.
11. Binh, P. C., Tri, N. M., Dung, D. T., Ahn, K. K., Kim, S. J., & Koo, W. (2016). Analysis, design and experiment investigation of a novel wave energy converter. *IET Generation, Transmission and Distribution, 10,* 460–469.
12. Do, H. T., et al. (2015). Effects of non-vertical linear motions of a hemispherical-float wave energy converter. *Ocean Engineering, 109,* 430–438.
13. Silvia, B., Adrià Moreno, M., Alessandro, A., Giuseppe, P., & Renata, A. (2013). Modeling of a point absorber for energy conversion in Italian seas. *Energies, 6,* 3033–3051.
14. Choi, K. S., Yang, D. S., Park, S. Y., & Cho, B. H. (2012). Design and performance test of hydraulic PTO for wave energy converter. *International Journal of Precision Engineering and Manufacturing, 13*(5), 795–801.
15. Tri, N. M., Binh, P. C., & Ahn, K. K. (2018). Power take-off system based on continuously variable transmission configuration for wave energy converter. *International Journal of Precision Engineering and Manufacturing-Green Technology, 5,* 89–101.
16. Binh, P. C., & Ahn, K. K. (2016). Performance optimization of dielectric electro active polymers in wave energy converter application. *International Journal of Precision Engineering and Manufacturing, 17,* 1175–1185.
17. Falnes, J., & Budal, K. (1978). Wave-power conversion by point absorbers. *Norwegian Maritime Research, 6*(4), 2–11.
18. Falnes, J. Principles for capture of energy from ocean waves. Phase control and optimum oscillation. http://folk.ntnu.no/falnes/web_arkiv/InstFysikk/phcontrl.pdf.
19. French, M. J. (1979). A generalized view of resonant energy transfer. *Journal of Mechanical Engineering Science, 21,* 299–300.
20. Guenther, D. A., Jones, D., & Brown, D. G. (1979). An investigative study of a wave-energy device. *Energy, 4*(2), 299–306.
21. Justino, P. A. P., Falcao, A. F. D. O. (2000). Active relief valve for an OWC wave energy devices. In *Proceedings of the European wave energy conference* (pp. 295–300).
22. Markus, R., Mario, E. M., Oliver, S., & Ted, K. A. B. (2014). Power optimisation of a point absorber wave energy converter by means of linear model predictive control. *IET Renewable Power Generation, 8,* 203–215.
23. Markus, R., Mario, E. M., Oliver, S., & Ted, K. A. B. (2013). Non-linear model predictive control of a point absorber wave energy converter. *IEEE Transactions on Sustainable Energy, 4,* 118–126.

24. Falnes, J. (2002). *Ocean waves and oscillating systems, linear interaction including wave-energy extraction*. Cambridge: Cambridge University.
25. Wang, H. T., & Lakes, R. S. (2004). Extreme stiffness systems due to negative stiffness elements. *American Journal of Physics, 72*(1), 40–50.
26. [Online] WAMIT version 7.0 user manual. http://www.wamit.com/manualupdate/history/V70_manual_old.pdf.
27. Jørgen, H. T. (2013). Practical limits to the power that can be captured from ocean waves by oscillating bodies. *International Journal of Marine Energy, 3–4,* e70–e81.

Publisher's Note Springer Nature remains neutral with regard to jurisdictional claims in published maps and institutional affiliations.
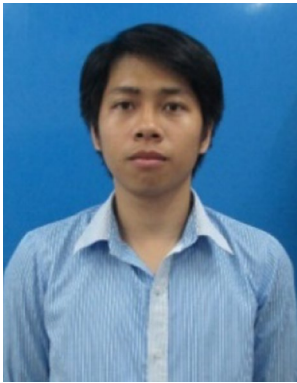
Tri Dung Dang received his B.S. degree in Mechatronics from Ho Chi Minh city University of Technology and Education, Viet Nam in 2013. He is now a Ph.D. candidate in Mechanical and Automotive Engineering in University of Ulsan. His research interests include robots, hydraulic system, renewable energy and automation.

Cong Binh Phan received his B.S. degree in Mechanical Engineering from Ho Chi Minh city University of Technical Education, Viet Nam in 2005 and the M.S. degree from Ho chi minh City University of Technology in 2009, and Ph.D. from the University of Ulsan, Korea in 2015. He is currently a lecturer in Mechanical department in Ho Chi Minh city University of Technology and Education, Viet Nam. His research interests involve in mechanical structural design, dynamic model and optimization the wave energy converter using smart material, hydraulic and mechanical power take-off system.

Kyoung Kwan Ahn received the B.S. degree from the Department of Mechanical Engineering, Seoul National University, Seoul, Korea, in 1990, the M.Sc. degree in mechanical engineering from Korea Advanced Institute of Science and Technology, Daejeon, Korea, in 1992, and the Ph.D. degree with the dissertation "A study on the automation of out-door tasks using 2 link electro-hydraulic manipulator," from Tokyo Institute of Technology, Tokyo, Japan, in 1999. He is currently a Professor in the School of Mechanical Engineering, University of Ulsan, Ulsan, Korea. His research interests include design and control of smart actuators using smart materials, fluid power control, and active damping control. Also, his works involve in design and control of wave energy converter using hydraulic and mechanical power take-off system.